

Original Article

Combined cell grafting and VPA administration facilitates neural repair through axonal regeneration and synaptogenesis in traumatic brain injury

Sujuan Liu¹, Haili Tian², Yanmei Niu³, Chunxia Yu⁴, Lingjian Xie⁴, Zhe Jin⁵, Wenyan Niu⁶, Jun Ren^{7,8,*}, Li Fu^{3,4,*}, and Zhi Yao^{6,*}

¹Department of Anatomy and Embryology, School of Basic Medical Science, Tianjin Medical University, Tianjin 300070, China, ²School of Kinesiology, Shanghai University of Sport, Shanghai 200438, China, ³Department of Rehabilitation, School of Medical Technology, Tianjin Medical University, Tianjin 300070, China, ⁴Department of Physiology and Pathophysiology, School of Basic Medical Science, Tianjin Medical University, Tianjin 300070, China, ⁵Tianjin Yaohua Binhai School, Tianjin 300000, China, ⁶Key Laboratory of Immune Microenvironment and Disease (Ministry of Education), Department of Immunology, School of Basic Medical Science, Tianjin Medical University, Tianjin 300070, China, ⁷Department of Cardiology, Zhongshan Hospital Fudan University, Shanghai Institute of Cardiovascular Diseases, Shanghai 200032, China, and ⁸Department of Laboratory Medicine and Pathology, University of Washington, Seattle, WA 98195, USA

*Correspondence address. Tel: +86-22-83336819; E-mail: yaozhi@tmu.edu.cn (Z.Y.) / Tel: +86-22-83336107; E-mail: lifu@tmu.edu.cn (L.F.) / Tel: +86-21-64041990; E-mail: jrenuwyo@126.com (J.R.)

Received 18 December 2021 Accepted 2 March 2022

Abstract

Neuronal regeneration and functional recovery are severely compromised following traumatic brain injury (TBI). Treatment options, including cell transplantation and drug therapy, have been shown to benefit TBI, although the underlying mechanisms remain elusive. In this study, neural stem cells (NSCs) are transplanted into TBI-challenged mice, together with olfactory ensheathing cells (OECs) or followed by valproic acid (VPA) treatment. Both OEC grafting and VPA treatment facilitate the differentiation of NSCs into neurons (including endogenous and exogenous neurons) and significantly attenuate neurological functional defects in TBI mice. Combination of NSCs with OECs or VPA administration leads to overt improvement in axonal regeneration, synaptogenesis, and synaptic plasticity in the cerebral cortex in TBI-challenged mice, as shown by retrograde corticospinal tract tracing, electron microscopy, growth-associated protein 43 (GAP43), and synaptophysin (SYN) analyses. However, these beneficial effects of VPA are reversed by local delivery of N-methyl-D-aspartate (NMDA) into tissues surrounding the injury epicenter in the cerebral cortex, accompanied by a pronounced drop in axons and synapses in the brain. Our findings reveal that increased axonal regeneration and synaptogenesis evoked by cell grafting and VPA fosters neural repair in a murine model of TBI. Moreover, VPA-induced neuroprotective roles are antagonized by exogenous NMDA administration and its concomitant decrease in the number of neurons of local brain, indicating that increased neurons induced by VPA treatment mediate axonal regeneration and synaptogenesis in mice after TBI operation. Collectively, this study provides new insights into NSC transplantation therapy for TBI.

Key words traumatic brain injury, transplantation, neural stem cells, valproic acid, N-methyl-D-aspartate

Introduction

Traumatic brain injury (TBI) is a devastating pathological condition with severe motor and neurological defects resulting from hypoxia-ischemia, cell damage/death, and proinflammatory responses [1–3]. TBI usually presents in two distinct forms, namely, primary and

secondary injuries. Many unfavorable outcomes are derived from secondary injury [4,5]. Among various therapeutic options, neural stem cells (NSCs) and olfactory ensheathing cells (OECs) were recently suggested to constitute novel cell therapeutic machineries against central nervous system (CNS) disease given their ability to

self-renew, differentiate into multiple target cells, secrete ample neurotrophic factors, and migrate towards damaged sites [2,3,6–8]. Accumulating evidence has depicted that NSC and/or OEC grafting may attenuate TBI through enhanced NSC differentiation into neurons to promote secretion of neurotrophic factors and protect against proinflammatory responses. Nonetheless, the precise mechanism of action behind NSC and OEC-evoked local neuronal improvement remains elusive in TBI mice.

Valproic acid (VPA, 2-propylpentanoic acid), a well-known histone deacetylase inhibitor, is widely used in the treatment of epilepsy and bipolar disorder [9–12]. Meanwhile, VPA is also utilized for the management of neurodegenerative disorders such as Alzheimer's disease through the inhibition of histone deacetylases [13]. More evidence suggests that VPA suppresses excitotoxicity-induced GAPDH nuclear accumulation and apoptotic death in neurons [14] and offers neurotrophic effects in various cell types, including midbrain dopaminergic (DA) neurons [15]. Recent finding has denoted that VPA may facilitate neuronal differentiation, although it suppresses astrocytic and oligodendrocytic differentiation of NSCs [16]. Despite the apparent neuroprotective role of VPA in CNS pathology, therapeutic mechanisms associated with VPA-induced induction of neuronal differentiation remain elusive. It was reported that the axon-sparing excitotoxin N-methyl-D-aspartate (NMDA) destroys local neurons in gray matter following its delivery into the peripherals of injured spinal cords [17]. In addition, NMDA was recently found to instigate retinal neurotoxicity and degeneration of retinal capillaries [18]. Notably, VPA overtly enhances NMDA receptor-mediated transmission and promotes plasticity in neocortex [19]. To this end, we hypothesize that the beneficial role of VPA may be associated with antagonism of NMDA.

In this study, we established a murine model of moderate controlled cortical impact (CCI) injury with motor and neurological dysfunction. Using this model, we found that combined transplantation of NSCs with OECs or VPA administration increased local neurons in the injured cerebral cortex, the effect of which was ablated following NMDA injection into surrounding tissues of the injury epicenter. Our results revealed that VPA promoted the differentiation of transplanted NSCs into neurons rather than astrocytes. Retrograde corticospinal tract tracing revealed that increased neurons could reconstruct broken neuronal circuits, and electron microscopic analysis revealed that increased neurons are accompanied by increased synaptic connections. Intriguingly, NMDA mitigated the increase in neurons in host brains and neural repair, suggesting a role of increased neurons in restoring the motor function of the injured cerebral cortex. These findings help to explain the precise mechanism behind the reversal of neurological functional impairment by elevation in neurons in brain-injured mice via neuronal gain- or loss-of-function strategies.

Materials and Methods

Primary culture of NSCs and OECs

NSCs and OECs were cultured, purified, and identified in following as described previously [2]. Hippocampal tissues harvested from C57BL/6 mouse embryos (E15–17 day; SPF Biotechnology Co., Ltd, Beijing, China) were used to culture NSCs; and olfactory bulb tissues of neonatal (1–3 days) C57BL/6 mice (SPF Biotechnology Co., Ltd) were used to culture OECs. In brief, the hippocampus or olfactory bulb tissues were cut into 1 mm³ pieces prior to the

formation of a cell suspension. The standard medium of NSCs contains Dulbecco's modified Eagle's medium/Nutrient Mixture F-12 (DMEM/F12; Gibco, New York, USA), 1% B27 (Gibco), 20 µg/L basic fibroblast growth factor (bFGF) (450-33-10; PeproTech, Offenbach, Germany), 20 µg/L epidermal growth factor (EGF) (315-09-100; PeproTech), and 1% penicillin/streptomycin (Gibco). Cells were then split at 90% confluency. After 3–5 passages, a portion of the single-cell suspension was plated onto glass cover slips coated with poly-L-lysine (Sigma-Aldrich, St. Louis, USA) for 12 h prior to fixation in 4% paraformaldehyde (PFA) for 20 min and stained with the mouse anti-Nestin (1:200, 66259-1-Ig; Proteintech) antibody for NSC identification. OECs were cultured in complete medium (DMEM/F12 supplemented with 10% fetal bovine serum) for 12 h. To remove fibroblasts for the purification of OECs, the cell suspension was transferred into a 24-well culture plate coated with poly-L-lysine for 24 h. OECs were then treated with 5 × 10⁻⁵ M arabinofuranosylcytosine (AraC) (HY-13605; MCE, New Jersey, USA) for 36 h. Following purification, OECs were fixed and stained with rabbit anti-p75-NGFR antibody (1:200, 55014-1-AP; Proteintech).

Differentiation assay *in vitro*

To induce NSC differentiation, NSCs were cultured for 2 days in complete medium containing 10% fetal bovine serum (FBS). To decipher the role of VPA in NSC differentiation, 0.5 mM VPA (P4543; Sigma-Aldrich) was administered to differentiation-induced NSCs for an additional 24 h. Cells were then fixed with 4% PFA for immunofluorescence staining using anti-NEUN (marker of mature neurons) and anti-GFAP (marker of astrocytes) antibodies.

Animal groups

All animal experiments were approved by the Animal Care and Use Committee of Tianjin Medical University (Tianjin, China). In brief, male C57BL/6 mice (8 weeks old, 22–25 g; JAX LAB, Bar Harbor, USA) were housed with food and water *ad libitum* in a 12-h light/dark cycle. Mice were randomly assigned to 7 groups as follows: (1) Sham group, mice with skull exposed only without weight impact; (2) TBI group, mice were subjected to controlled cortical impact operation while receiving saline; (3) OEC group, TBI mice were subject to an equal volume of OEC transplantation; (4) NSC group, TBI mice were subject to an equal volume of NSC transplantation; (5) VPA group, simultaneous treatment of TBI model mice that received NSC transplantation and VPA intraperitoneal injections (150 mg/kg); (6) NMDA group, a cohort of VPA mice that received NMDA (5 µL/site, 10 mM; MCE) injections into 4 local sites around the injury epicenter in the brain; and (7) in the CO group, TBI mice were co-transplanted with equal volumes of NSCs and OECs.

TBI model

A controlled cortical impact device (eCCI Model 6.3; VCU, Richmond, USA) was used to establish TBI. In brief, mice were anesthetized and placed in a stereotaxic frame. A 5-mm hole over the right cerebral cortex was made using a portable drill. Mice were subject to CCI at a velocity of 6 m/s, a depth of 0.6 mm, and a 150-ms impact duration using a device with a 2.5-mm flat-tip impounder. The scalp was sutured, and the mice were returned to their cages and monitored for at least 4 h following surgery. Sham mice received similar treatment except impact.

Cell transplantation, VPA and NMDA injection

Prior to transplantation, NSCs and OECs were incubated for 30 min in medium containing CM-Dil (red; Yeasen, Shanghai, China) and Hoechst 33342 (blue; Sigma-Aldrich), respectively. Cells were re-suspended at a final concentration of 1×10^7 cells/mL in DMEM/F-12. A glass micropipette connected to an electric stereotaxic Ultra Micro Pump III (UMP3) instrument (WPI, Sarasota, USA) was used for cell transplantation. Suspended cells were engrafted around the injury epicenter of the brain through 4 local sites (5 μ L/site) at a rate of 1 μ L/min. A combination of 50% NSCs and 50% OECs was grafted as a CO group, ensuring an equal number of cells in each group. Mice from the TBI groups received only saline injection. Mice from the VPA group were given a daily intraperitoneal injection of VPA (150 mg/kg; Sigma-Aldrich) beginning from 7 days post-operation (dpo) for 7 additional days. NMDA (5 μ L/site, 10 mM; MCE) or saline was delivered using the UMP3 instrument into 4 local sites around the injury epicenter of the brain at 14 dpo.

Behavioral testing

Behavioral testing was performed at 0, 7, 14 and 21 dpo. The neurological severity score [20], the wire hanging test [21], and the grid walking test [22] were employed to evaluate neurological, forelimb motor, and skeletal muscle function, respectively. The modified neurological severity score (mNSS), including 18 scales of scores (normal: 0; maximal deficit: 18), was employed to assess motor, sensory, and reflex function. A higher score suggests worsened neurological function. The wire hanging test is sensitive to defects in global skeletal muscle. In brief, a stainless steel bar (50 cm length, 2.0 mm diameter) was rested on two vertical stands (37 cm above the floor). Each mouse was hung onto the middle portion of the bar with two forepaws. The hanging time was recorded until mice fell in 4 parallel tests (30 s/test). 0 score: fall in less than 30 s; 1 score: tightly grasp the bar with two forepaws; 2 score: tightly grasp and try to climb the bar; 3 score: tightly grasp the bar with two forepaws and one (or two) hindpaw (s); 4 score: tightly grasp the bar with all fours and tail; 5 score: escape to one side of the apparatus in less than 30 s. The grid walking test was employed to detect defects in descending motor control. Each mouse was placed on a stainless steel grid approximately 40 cm \times 20 cm \times 50 cm (length \times width \times height) with a mesh size of 2 cm \times 2 cm. Behavior was videotaped for 3 parallel tests (1 min/test). A step that failed to provide support and went through the grid hole was considered a foot fault. Total foot faults of contralateral forelimbs and the total number of forelimb steps were recorded. All behavioral tests were performed in a blinded manner.

Double immunofluorescence staining

Double immunofluorescence staining was performed at 21 dpo *in vivo*. Cells or brain tissues were fixed for 24 h in 4% PFA, and brain tissues were then dehydrated with 20% sucrose (Sigma-Aldrich) at 4°C overnight. Brain tissues were serially sliced horizontally into 12- μ m-thick sections using a freezing microtome (CM1900; Leica, Wetzlar, Germany). Fixed cells or brain sections were stained with mouse anti-NEUN (1:200, EPR12763; Abcam, Cambridge, USA) and rabbit anti-GFAP (1:100, 0190-1-Ig; Proteintech) antibodies at 4°C overnight. After washing, the samples were incubated for 60 min at 37°C with a fluorescence-labelled secondary antibody IgG, such as anti-rabbit Alexa Fluor 488 (1:100, ab150077; Abcam) and anti-

mouse Cy3 (1:100, BA1031; Boster) antibodies. Sections were incubated in phosphate-buffered saline (PBS, 0.01 M; Sigma-Aldrich) to replace the primary antibodies as a control. Following DAPI staining (36308ES11; Yeasen), slides were mounted and visualized with a fluorescence microscope (DM RBE; Leica). All data were collected from at least 15 images from 3 individuals (5 images per area) or 3 consecutive sections per animal for all groups in parallel experiments.

Retrograde corticospinal tract tracing

To quantify the sparing/regeneration of the surrounding corticospinal tract in the injured brain, retrograde labelling procedures were performed at 14 dpo. Mice were anesthetized, and the T12 vertebra was exposed by laminectomy. Five microliters of retrograde trace fluoro-gold (FG, 4%; Fluorochrome, Denver, USA) was bilaterally microinjected into the spinal cord 0.1 mm lateral to the spinal midline by the electric stereotaxic UMP3 instrument. All procedures were performed by the same person. The brain was dissected and coronally sliced into 15- μ m sections 7 days after FG injection. Brain sections were rapidly photographed with the fluorescence microscope and analysed using ImageJ software. Labelled FG neurons were counted from 5 fields in 3 sections from each mouse in a blinded manner.

Electron microscopy

Double electron microscopy was performed at 21 dpo. Mice were transcardially perfused with phosphate buffer (PB, 0.1 M) containing glutaraldehyde (2.5%) and PFA (2%) at 21 dpo. The brain tissues were removed and postfixed in the same fixative at 4°C overnight. The right cerebral cortex was sliced into 60- μ m coronal sections using a vibrating blade microtome (VT1000s; Leica) for the electron microscopy experiment as described previously [23]. Briefly, tissues were incubated in PB (0.1 M) supplemented with OsO₄ (1%) for 1 h, dehydrated with an ascending ethanol series, and finally embedded in epoxy resin through propylene oxide. The ultrathin sections were obtained using an ultramicrotome (Ultracut N; Leica) placed on formvar-coated 1-hole Cu grids. Images of synapses were visualized using a transmission electron microscope (H-7650; Hitachi, Tokyo, Japan). At least 15 images were analysed using ImageJ software.

Immunohistochemistry

Immunohistochemistry was conducted at 21 dpo from at least 3 independent brain tissue sections (15 μ m). Brain samples were fixed and dehydrated as described in the previous immunofluorescence staining section. Growth-associated protein 43 (GAP43) antibody (1:300, 16971-1-AP; Proteintech) was used to assess axonal regeneration in the host brain. A synaptophysin (SYN) antibody (1:300, 17785-1-AP; Proteintech) was used to detect synaptogenesis and synaptic plasticity. Sections were incubated with diluted primary antibodies overnight at 4°C, followed by incubation with HRP-conjugated anti-rabbit secondary antibody (1:200, #8114; CST, Denver, USA). Finally, images of the sections were observed and captured with a light microscope (CTR6000; Leica). At least 15 images from 3 consecutive sections per animal for all groups were used in the statistical analysis.

Statistical analysis

All data are expressed as the mean \pm SEM. Unpaired Student's 2-

tailed *t* test was used for comparison between 2 experimental groups, and two-way ANOVA followed by Tukey's *post hoc* test was employed for multiple group comparison. $P < 0.05$ was considered to be statistically significant.

Results

VPA treatment promotes neuronal differentiation of primary NSC cultures

Given the established role of VPA in the induction of neuronal differentiation of NSCs in the injured CNS [24,25], VPA was administered to primary cultured NSCs. First, we cultured NSCs and OECs. Neurosphere formation was observed 2–3 days after plating, accompanied by increased number and size following 5–6 days of culture and evident nestin-positive staining (green) following 3–5 passages (Figure 1A, top). In addition, a high volume of bipolar and multipolar cells with long and thin processes were identified, exhibiting a mosaic monolayer arrangement following adherent culture and AraC treatment. OECs were visualized using immunofluorescence staining with the p75-NGFR antibody, while positive staining (green) was confirmed as OECs (Figure 1A, bottom). To

trace the fate of engrafted cells, NSCs and OECs were labelled with CM-Dil (red) and Hoechst 33342 (blue), respectively, prior to transplantation (Figure 1A). To determine whether VPA provokes neuronal differentiation, NSCs were pretreated for 2 days in complete medium supplemented with 10% FBS prior to exposure to VPA (0.5 mM) for an additional 24 h. The results revealed more abundant NEUN-positive cells and fewer GFAP-positive cells following VPA treatment (Figure 1B–D), suggesting the ability of VPA administration to drive NSC differentiation into neurons as opposed to astrocytes.

Cell grafting and VPA promote neurological functional recovery, whereas NMDA eliminates the effects of VPA

To explore the impact of cell grafting and VPA administration on TBI, NSCs and/or OECs were delivered into the surrounding epicenter of CCI-induced TBI brain injury prior to VPA administration with or without NMDA injection (Figure 2A). Our data noted the presence of red and blue fluorescence in the host cerebral cortex 21 days after cell transplantation, suggesting that implanted NSCs and OECs survived and spread across the host brain (Figure 2B). At

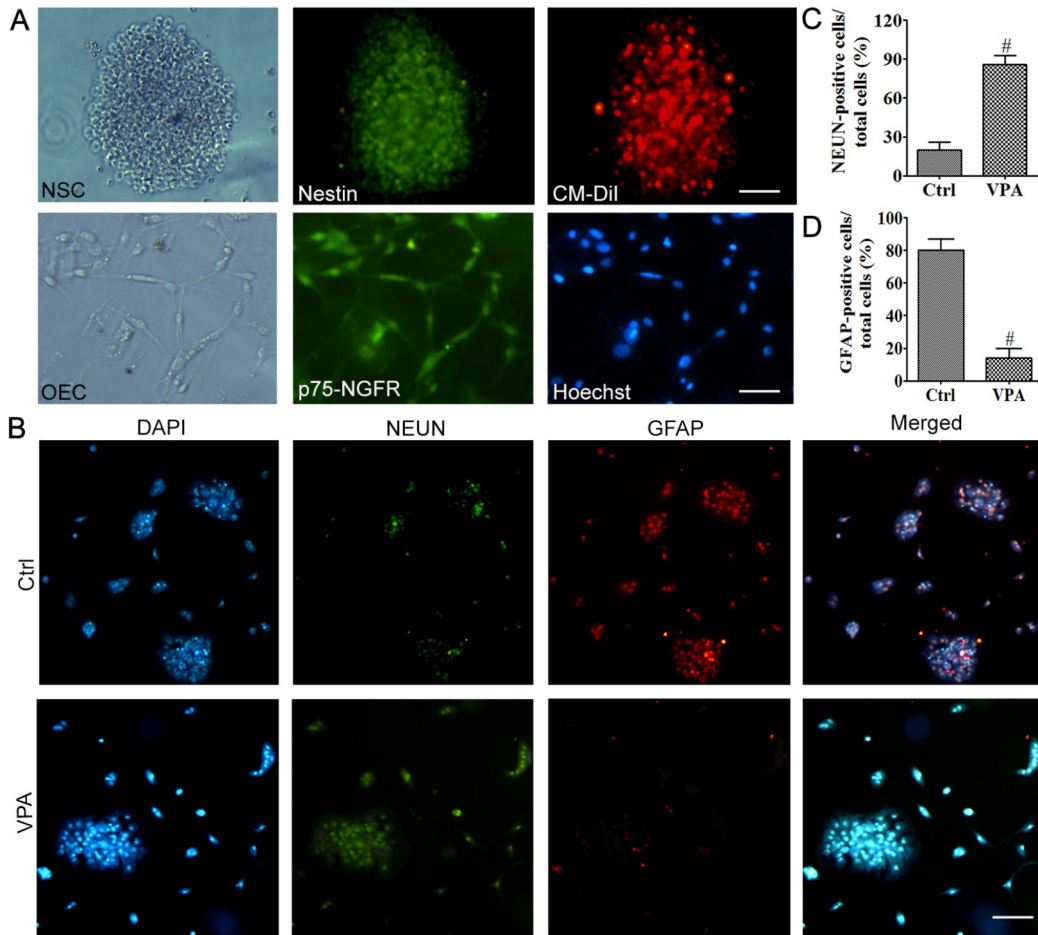


Figure 1. VPA treatment promotes neuronal differentiation of primary cultures of NSCs (A) Representative images of primary cultures of NSCs (top) and OECs (bottom) *in vitro*. NSCs in neurosphere formation, Nestin-positive stained (green) and labelled by CM-Dil (red) before transplantation; OECs have a shuttle appearance, p75-NGFR-positive stained (green) and labelled by Hoechst 33342 (blue) before transplantation. Scale bar: 30 μm . (B) Representative images of NSC differentiation induced by VPA treatment. VPA (0.5 mM) was administered to NSCs 24 h after differentiation induced by 10% FBS for 2 days. NSCs were fixed and stained. Scale bar: 50 μm . (C,D) Relative quantification of positive staining of NEUN (C) and GFAP (D) with or without VPA treatment in NSCs. All data shown are from at least 15 images from 3 individuals (5 images per area) in parallel experiments. $^{\#}P < 0.01$.

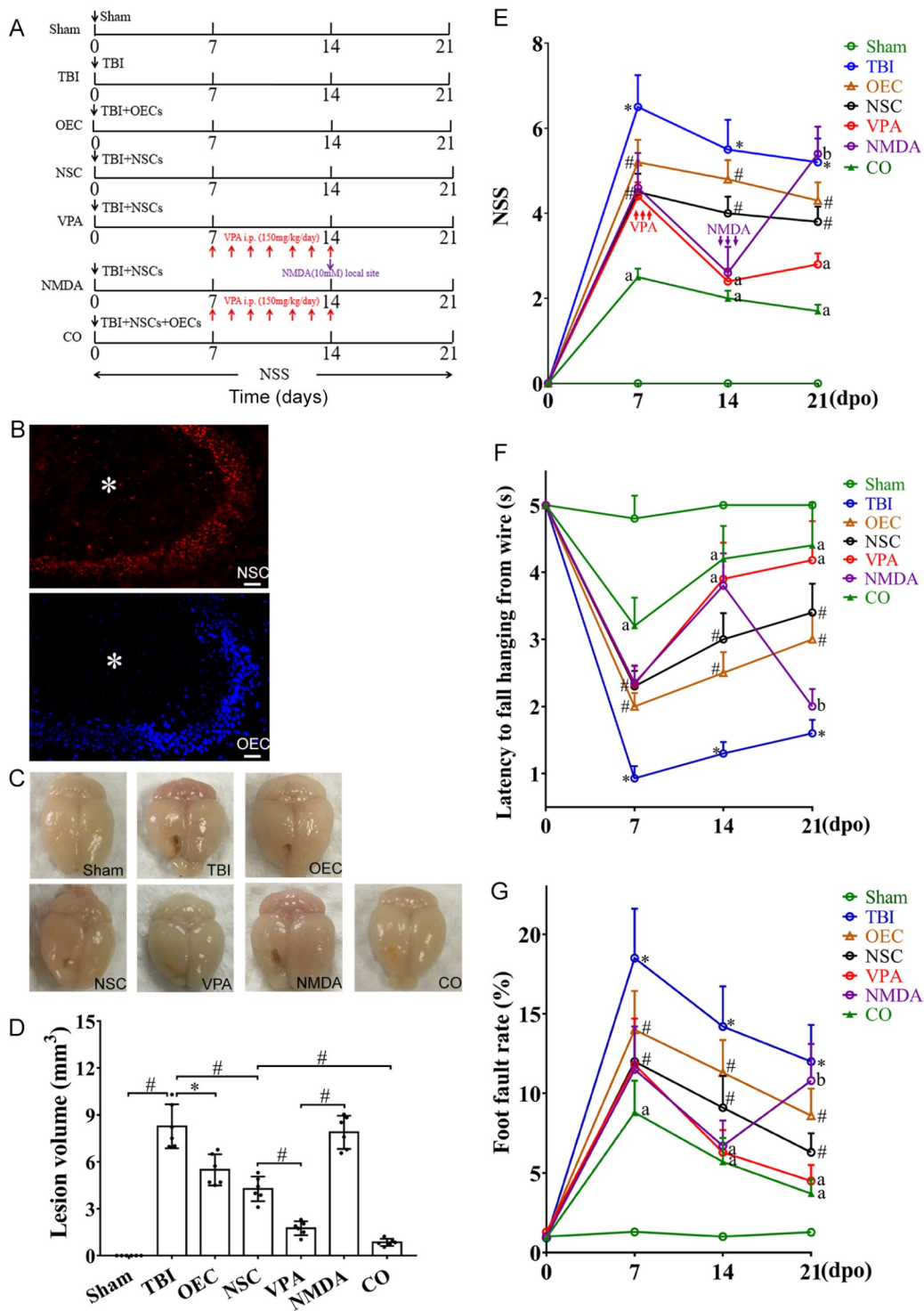


Figure 2. Cell grafting and VPA promote neurological functional recovery, whereas NMDA eliminates the effects of VPA (A) Schematic flow chart of surgical procedures, cell transplantation and VPA and NMDA injection. (B) Implanted NSCs and OECs emit red (CM-DiI, scale bar: 50 μm) and blue (Hoechst 33342, scale bar: 30 μm) fluorescence in the host cerebral cortex at 21 dpo, respectively. The injury epicenter of the cerebral cortex is denoted with (*). (C,D) Representative images (C) and lesion volume quantification of the brains (D), treated as indicated, at day 21 after TBI, OEC grafting, NSC grafting, NSC grafting and VPA administration with or without NMDA; co-grafting NSC and OEC treatment (n=6). *P<0.05; #P<0.01. (E) The changes in NSS at 0, 7, 14, and 21 days after TBI operation. (F) The time of hanging was recorded until the mice fell in the wire hanging test. For each mouse, 4 parallel experiments were performed. (G) Quantification of the foot faults in mice after TBI operation, cell transplantation and VPA and NMDA injection. The data were expressed as a percentage of total steps by the foot fault number of the forelimbs in injured contralateral. (E,F) Data are presented as the mean ± SEM (n=6). *P<0.01 vs sham; #P<0.05 vs TBI; ^aP<0.05 vs NSC; ^bP<0.01 vs VPA.

21 days post-CCI injury, brain samples were collected, and the lesion volume was quantified as shown in Figure 2C,D. The injured volume of the motor cortex was larger in TBI mice than in sham mice, the effect of which was attenuated or reconciled following NSC and/or OEC transplantation and VPA treatment. Intriguingly, the beneficial effects of VPA against TBI were mitigated by NMDA (Figure 2C,D). To evaluate whether the changes in brain morphology affect behavioral responses, neurological, forelimb motor, and skeletal muscle functions were examined. Consistent with previous reports [2,3], TBI operation led to a significantly higher NSS compared with sham-treated mice. Compared with the TBI group,

NSS was significantly decreased in OEC and/or NSC treatment groups 7 and 21 dpo. In addition, NSS was overtly decreased following combined NSC transplantation and VPA treatment at 14 and 21 dpo in comparison with mice from the NSC transplantation alone group after TBI. This beneficial effect of VPA was reversed by NMDA (Figure 2E). Similar results were obtained in forelimb motor and skeletal muscle functions (Figure 2F,G). These findings indicated that TBI injury results in neurological, motor, and skeletal muscle functional impairments in mice, the effects of which were improved by cell transplantation and VPA treatment, especially with NSC and OEC co-transplantation.

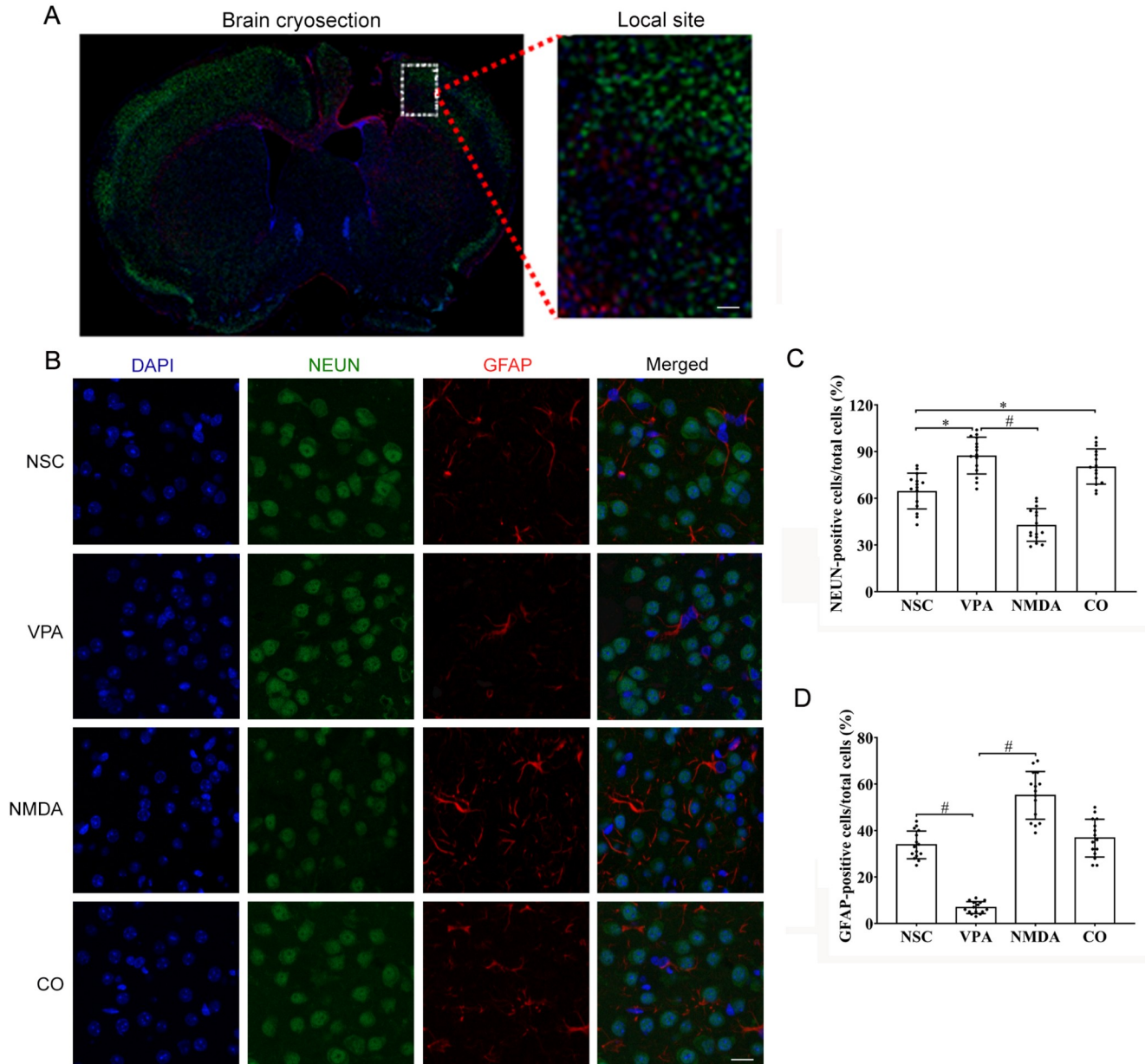


Figure 3. VPA or OECs drives NSC differentiation into neurons *in vivo*, whereas NMDA negates the beneficial effects of VPA (A) Sagittal cryosection of injured brain stained with anti-NEUN (green) and anti-GFAP (red) antibodies, and high-magnification image of local site in the white rectangle. Scale bar: 50 μm . (B) Representative images of brain sections stained with anti-NEUN (green), anti-GFAP (red) and DAPI (blue) after cell transplantation and VPA and NMDA injection. Scale bar: 20 μm . (C, D) The percentages of NEUN (C) or GFAP (D)-positive cells in the total cells were quantified. All data shown are from at least 15 images from 3 individuals (5 images per area) in parallel experiments, and presented as the mean \pm SEM. * $P < 0.05$; # $P < 0.01$.

VPA or OECs drives NSC differentiation into neurons *in vivo*, whereas NMDA negates the beneficial effects of VPA

We further evaluated the effects of VPA, NMDA, and OECs on NSC differentiation in localized brain injury sites using double immunofluorescence (Figure 3A). Brain samples were collected from four treatment groups, including NSC, VPA, NMDA, and CO. Our data showed that the number of NEUN-positive cells in the host was significantly increased in the VPA and CO groups compared with that in the NSC group, suggesting enhanced neuronal differentiation by NSCs in combination with VPA administration or OEC grafting in TBI mice (Figure 3B,C). However, NMDA overtly offset the VPA-induced response in NEUN-positive cells (Figure 3B,C). Conversely, combined NSCs with VPA administration led to an overt decrease in GFAP-positive cells in the brain, the effect of which was reversed by NMDA injection (Figure 3B,D). In addition, little discernable difference was noted in the number of GFAP-positive cells in brains

between the NSC and CO groups (Figure 3B,D). Therefore, *in vivo* VPA administration seems to drive the differentiation of NSCs into neurons as opposed to astrocytes (Figure 3), consistent with our findings *in vitro* (Figure 1B–D). These data indicated that VPA or OEC treatment drives NSC differentiation into neurons *in vivo*, whereas local NMDA delivery into the brain ablates the VPA-induced beneficial effect, resulting in significant impairment of neuronal functions.

Combining NSCs with OECs or VPA enhances axon extension, whereas the VPA-induced response is reversed by NMDA

To elucidate functional variance, we explored the possible effect of cell grafting, VPA, and NMDA administration on the restoration of neuronal function. Trace FG was retrogradely microinjected into the spinal cord at T12, and the FG-labelled cells surrounding the epicenter brain injury is shown in Figure 4A–D. After CCI injury, the

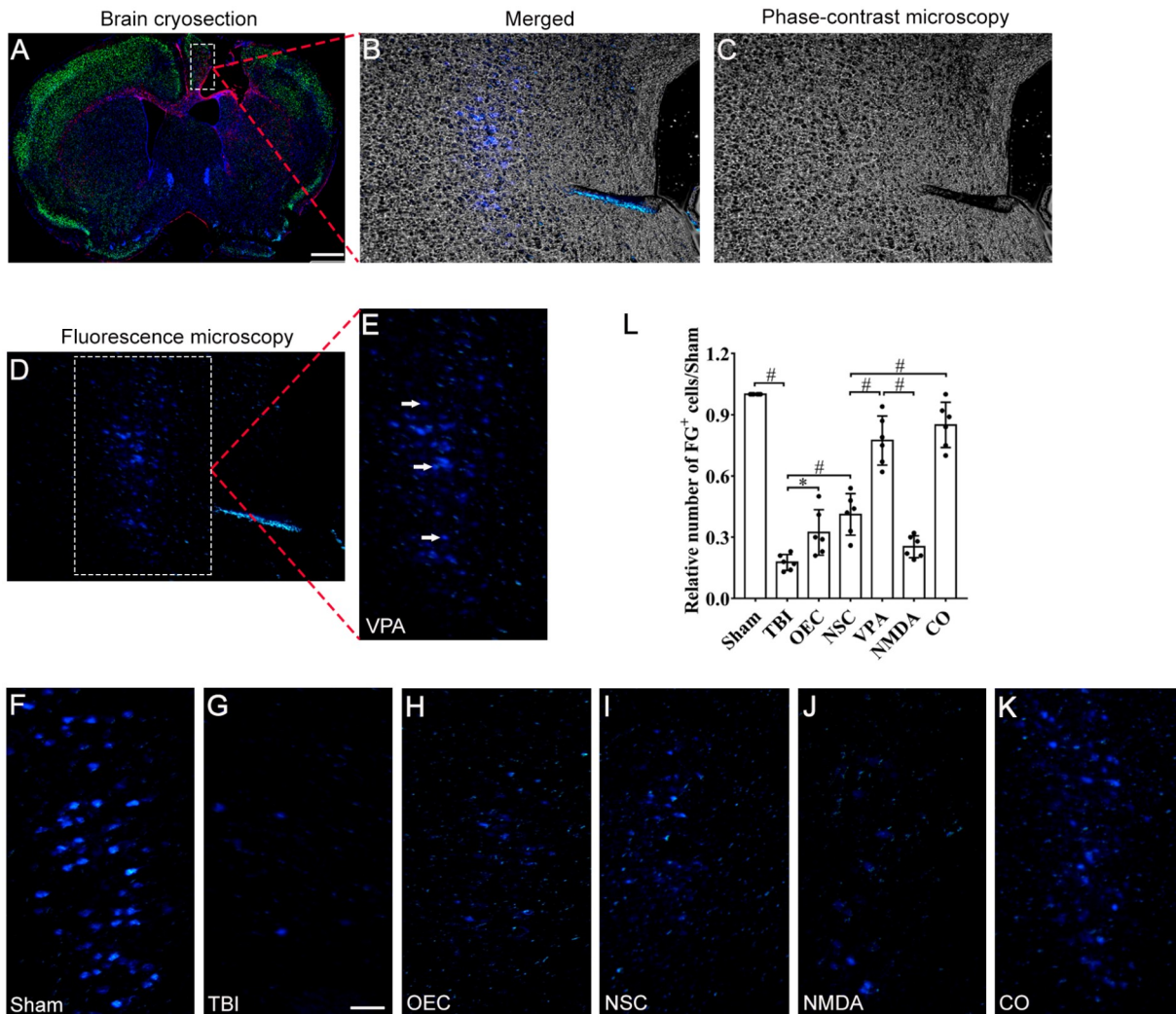


Figure 4. Combining NSCs with OECs or VPA enhances axon extension, whereas the VPA-induced response was reversed by NMDA (A–D) Brain cryosection (A) and high-magnification image of the local site in the white rectangle shown in (B), which was merged by the phase-contrast image (C) and fluorescence image (D). Scale bar: 200 μ m. (E–L) Representative high-magnification images (E–K) and quantification (L) of FG-positive cells in mouse brains from sham operation (F) TBI operation (G), OEC grafting (H), NSC grafting (I), NSC grafting and VPA administration with or without NMDA (J), and cografing NSC and OEC treatment (K) shown as indicated. Scale bar: 50 μ m. Arrows indicate FG-positive cells. Three brain sections from each animal and at least six mice from each group were analysed. Data are presented as the mean \pm SEM ($n=6$). * $P<0.05$; # $P<0.01$.

number of FG-labelled cells was approximately 5 folds lower in the host brain than in the sham-operated group (Figure 4F,G,L). Compared with that in the TBI group, the number of FG-labelled cells in the host brain was significantly increased in the OEC and NSC groups (Figure 4G–I,L). Moreover, combined grafting of NSCs and OECs resulted in a significant increase in FG-positive cells in brains compared with that from NSC or OEC transplantation alone (Figure 4H,I,K,L). VPA significantly increased the number of FG-positive cells in the brain, the effect of which was reversed by local injection of NMDA (Figure 4E,I,J,L). Our results suggested that combined OECs or VPA with NSCs promoted axonal outgrowth in the host brain of CCI-injured mice. However, NMDA injection nullified the beneficial effect of VPA and prevented axonal extension in the injured brain, which may be attributed to NMDA-induced increase in astrocytes (Figure 3B,D). These data indicated that combining NSCs with OECs or VPA enhances axon extension, whereas the VPA-induced response is reversed by NMDA.

Effect of cell grafting, VPA, and NMDA intervention on axonal regeneration in the brain

To further assess axonal regeneration in the host brain, GAP43 was detected in brain sections following cell grafting, VPA and NMDA administration. IHC results revealed significantly reduced GAP43-positive staining following TBI injury (Figure 5A,B,H), denoting serious axonal damage. GAP43 was overtly elevated in the brain

following NSC and OEC treatment alone or in combination (Figure 5B–D,G,H). No significant difference was observed in GAP43-positive staining between the NSC and OEC groups, although concurrent transplantation of NSCs and OECs significantly upregulated GAP43 levels in the host brain compared with single grafting of either one alone (Figure 5C,D,G,H). In addition, intraperitoneal injections of VPA after NSC grafting resulted in a prominent rise in GAP43 in the brain (Figure 5D,E,G). Nonetheless, NMDA reversed the VPA-induced beneficial effect of GAP43 against CCI-injured TBI (Figure 5E,F,H). These data indicated that NSC and/or OEC grafting and VPA administration increased axonal regeneration in the brain of TBI mice, but this beneficial effect of VPA was reduced by NMDA administration.

Effect of cell grafting, VPA, and NMDA administration on synaptic number in the cerebral cortex

The number of synapses was monitored following cell grafting and VPA and NMDA administration in the host brains of mice. Electron microscopy results showed that the TBI procedure led to an overt drop in the number of synapses in the host brain, the effect of which was reversed by cell grafting into the injured brain, including NSCs, OECs, and NSCs along with OECs (Figure 6A–D,G,H). Although little difference was observed in the number of synapses in brains between the OEC and NSC groups, the CO group possessed an overtly higher number of synapses than OEC or NSC treatment

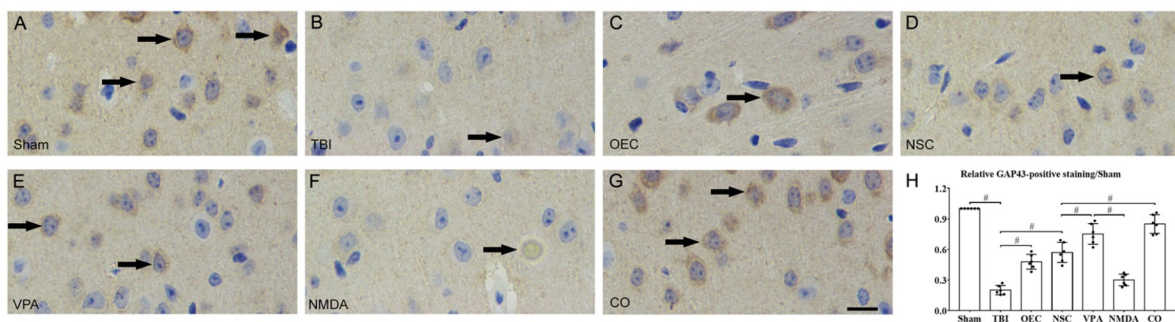


Figure 5. Effect of cell grafting, VPA, and NMDA intervention on axonal regeneration in the brain (A–H) Representative images (A–G) and quantification (H) of GAP43-positive cells in mouse brain sections from sham control (A), TBI operation (B), OEC grafting (C), NSC grafting (D), NSC grafting and VPA administration (E) or plus NMDA (F), and cografting NSCs and OEC treatment (G) treated as indicated. Scale bar: 20 μ m. Arrows indicate GAP43-positive stained cells in the brain. Data are presented as the mean \pm SEM ($n=6$). $^{\#}P<0.01$.

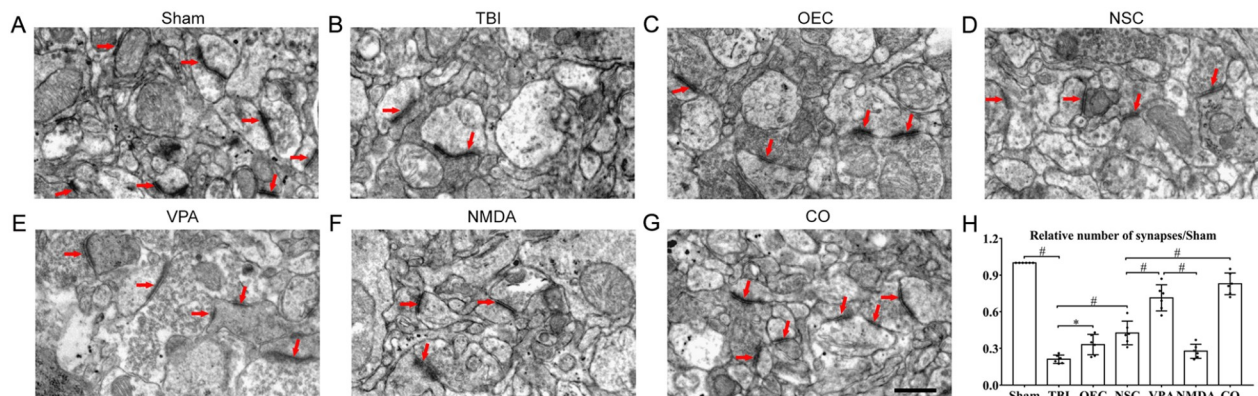


Figure 6. Effect of cell grafting, VPA, and NMDA administration on synaptic number in cerebral cortex (A–H) Representative electron microscopy images (A–G) and quantification (H) of synaptic connection in brain sections after TBI operation (B), cells grafting (C,D,G) and VPA (E) or NMDA (F) injection treatment, shown as indicated. Arrows indicate synapses in neurons of brain tissue. Scale bar: 1 μ m. Data are presented as the mean \pm SEM ($n=6$). $^*P<0.05$; $^{\#}P<0.01$.

alone (Figure 6C,D,G,H). As expected, VPA administration overtly increased synapses and promoted their connectivity in neurons, the effect of which was reversed by NMDA injection (Figure 6D–F,H). Our data demonstrated that NSC and/or OEC grafting and VPA administration increased the number of synapses in TBI mice, but this trend was reversed by NMDA.

Synaptogenesis and synaptic plasticity in response to NSC/OEC transplantation, VPA and NMDA injection

Synaptogenesis and synaptic plasticity are required for neuronal function and activity in the CNS, and their defects contribute to neurological disorders such as autism and epilepsy [26,27]. We next examined the expression of SYN to evaluate alterations in synapses in cortical neurons following NSC and/or OEC grafting, VPA and NMDA administration. Compared with the sham group, SYN-positive staining was significantly decreased in the host brain from the TBI group (Figure 7A,B,H). Similar to the results for GAP43, SYN was markedly increased in the brains from all cell grafting groups, especially the CO group (Figure 7B–D,G,H). VPA treatment significantly increased SYN expression in the brains of transplanted NSC mice, the effect of which was mitigated by local injection of NMDA into the surrounding area of the injured brain (Figure 7D–F, H). These data indicated that NSC and/or OEC grafting and VPA administration increased synaptogenesis and synaptic plasticity in the cerebral cortex in TBI-challenged mice, while this trend was reversed after NMDA injection.

Discussion

TBI disrupts brain function and circuitry and is accompanied by pathological changes, including neuronal death [2,3,19,28–30], axonotmesis [3,31], and scar formation [32]. In this study, our results indicated that the loss of brain tissue was prominent, along with neurological, skeletal muscle, and motor defects, in TBI mice. However, given the moderate severity of TBI injury, neurological, skeletal muscle, and motor functions may be spontaneously recovered at 14 dpo and 21 dpo. Moreover, our data showed that CCI injury led to a pronounced drop in FG-positive cells and GAP43 levels in the cerebral cortex, denoting axonal damage in brains in the TBI model. Moreover, the number of synapses was markedly

decreased in the cerebral cortex of TBI mice, as assessed by electron microscopy. In addition, a similar trend of SYP-positive cells was noted in TBI mouse brains, denoting defective synaptic function and synaptogenesis following the TBI procedure. Therefore, such a CCI injury model should enable us not only to examine the pathogenesis of the disease process but also to develop possible therapeutic remedies for TBI.

Findings from our lab and others have revealed overtly dropped neurons in host brains with CNS diseases, including TBI and spinal cord injury (SCI) [2,3]. As a measure to reconcile neuronal damage, cell regeneration has shown some promise in TBI and spinal cord injury, although CNS regeneration is rather challenging due to cell-intrinsic plasticity reduction induced by neuronal death or dysfunction at CNS injury sites [33,34]. These findings suggest that local neurons at the injured CNS sites play an important role in neuronal regeneration and restoration. Recent studies have demonstrated the use of cell transplantation, such as NSCs, bone mesenchymal stem cells (BMSCs), OECs and Schwann cells (SCs), in restoring the number of neurons in the host through secretion of neurotrophic factors, induction of neuronal differentiation, and anti-inflammatory events [2,3,34,35]. To further investigate the efficacy of cell grafting on neural restoration, NSCs and OECs, either independently or in combination, were delivered into brain regions surrounding the injury. Behavioral tests, retrograde corticospinal tract tracing, electron microscopy and immunohistochemistry were then performed to monitor the effect of cell grafting following TBI. Our data revealed that NSC or OEC transplantation improves neurologic and motor functions accompanied by axonal regrowth, synaptogenesis, and synaptic plasticity in brain injury. More intriguingly, co-transplantation of NSCs and OECs exerted a better therapeutic and synergistic efficiency against CCI-injury than either NSCs or OECs alone. These findings suggest that co-transplantation of NSCs and OECs instigates a significant increase in neurons from the host brain, likely due to improved NSC survival in injury sites and induction of the differentiation of engrafted NSCs into neurons following OEC administration. Given that the apoptosis of neurons evoked by CNS anomalies is usually detrimental and irreversible, the maintenance of survival for neurons derived from NSC transplantation is essential for tissue repair in CNS injury sites. To

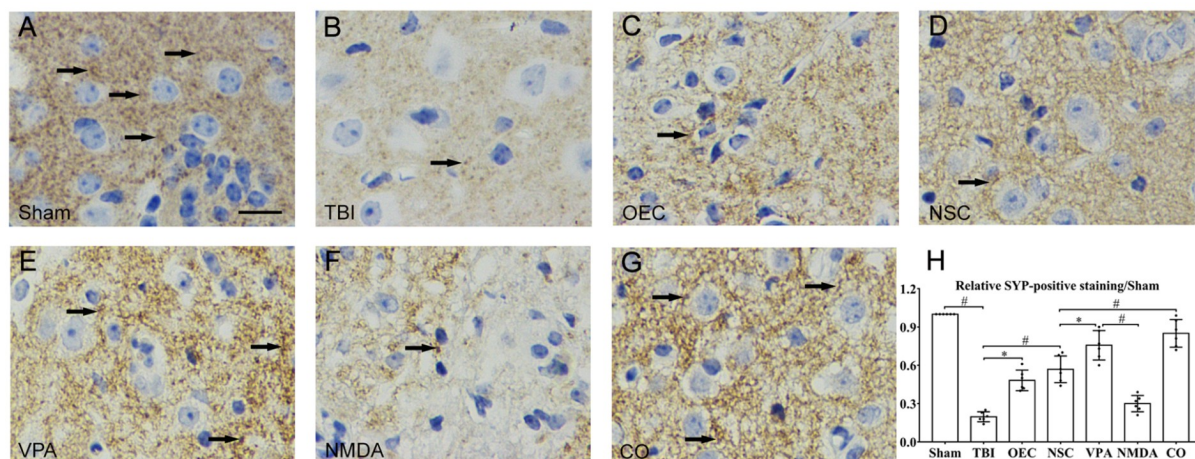


Figure 7. Synaptogenesis and synaptic plasticity in response to NSC/OEC transplantation, VPA and NMDA injection (A–H) Representative images (A–G) and quantification (H) of SYP-positive cells in mouse brains from sham control (A), TBI operation (B), OEC grafting (C), NSC grafting (D), NSC grafting and VPA administration (E) or plus NMDA (F), and co-grafting NSC and OEC treatment (G) shown as indicated. Arrows indicate SYP-positive cells. Scale bar: 20 μ m. Data are presented as the mean \pm SEM ($n=6$). * $P<0.05$; # $P<0.01$.

this end, preservation of local neurons in brain injury is believed to play a vital role in axonal regrowth, synaptogenesis, and synaptic plasticity, as evidenced by functional recovery from cell grafting in TBI mice in the current study.

Earlier findings have reported that VPA evokes neuronal differentiation, although it suppresses astrocytic and oligodendrocytic differentiation of NSCs [16]. Consistent with previous findings, our data also confirmed that VPA administration triggers the differentiation of engrafted NSCs into neurons rather than astrocytes *in vitro* and *in vivo*. Recent evidence has also indicated that the proliferation of astrocytes in the CNS is closely associated with scar formation to restrict axonal regeneration [36,37]. Furthermore, our results showed that combined NSC grafting and VPA administration promoted functional recovery of TBI mice and favored axonal regrowth, synapses, and synaptic plasticity in the host. Our observation is consistent with a recent report that VPA treatment increases SYN immunostaining in the medial prefrontal cortex [26]. These data indicated that OEC grafting and VPA administration play a similar beneficial role in the functional recovery of NSC-transplanted mice, and their synergistic effects in ameliorating TBI injury are prominent. A rise in endogenous and transplant-derived neurons is considered a major factor for functional recovery of TBI. The reconstruction of neurons is believed to be responsible for the reconstruction of broken neuronal networks for several reasons: (1) the transplant-derived neurons would receive projections from endogenous neurons to extend synaptic processes with endogenous neurons in host brains; and (2) neurons may be reconstructed in disrupted corticospinal tract.

Our data showed that NMDA injection into the brain mitigated the beneficial effects of VPA in TBI injury, as revealed by retrograde corticospinal tract tracing, electron microscopy analysis, and immunohistochemistry. NMDA has been shown to trigger neuronal injury due to NMDA-induced neuronal excitotoxicity, cell injury, and apoptosis in various tissues, including the cerebral cortex [38,39], retina [18,40,41], hippocampus [42], and spinal cord [7]. Glutamate (Glu) acts on glutamate receptors, such as NMDA receptors (NMDARs), and leads to neuronal hyperexcitability and death in a dose-dependent manner [43]. Moreover, Abematsu *et al* [7] showed that NMDA injection reversed spontaneous and treatment-provoked functional recovery after SCI, indicating that NMDA induced functional loss of neurons, suggesting an important role for endogenous and transplant-derived local neurons in the restoration of hind limb motor function [7]. Other than ablation of local neuronal function [7,38,40], NMDA injection also induced an increase in astrocytes but not neurons in the NSC-transplanted mouse brain. Our results are consistent with recent reports of a vital role of local neurons in the functional recovery of spinal cord injury [44,45]. In our study, NMDA was injected into the area surrounding the epicenter injury to ablate the function of local brain neurons. In this loss-of-function neuron model induced by NMDA, the possible role of local neuronal neurogenesis and repair may be deciphered following TBI. VPA was shown to foster transmission and increase plasticity in neocortex through NMDAR [19]. VPA also limits NMDA-induced increases in K^+ and eicosanoid levels and inhibits glutamatergic activity in the bipolar disorder diseased brain [46]. In addition, VPA was shown to protect neurons against NMDA through various mechanisms, including neuronal TrkB receptor [47] and ERK [48]. Furthermore, the beneficial effects of VPA on functional recovery after SCI were mitigated by NMDA injection [7].

Consistent with previous reports, our data showed that increased neurons by NSC transplantation and VPA treatment were markedly reduced following NMDA injection. Meanwhile, the restoration and improvement of motor and neurological functions following NSC and VPA treatment were also reversed following NMDA administration. Our data reinforced those previous findings that NMDA leads to the neuronal hyperexcitability and death in the CNS [39,41] and that VPA is beneficial and neuroprotective for the CNS lesions [24,25,49].

In summary, our findings revealed that co-administration of NSCs and OECs or VPA evoked neuronal differentiation and reconciled neuronal function impairments induced by TBI, accompanied by enhanced axonal regrowth, increased synapses and synaptic plasticity in the host brains. Intriguingly, these beneficial effects were reversed by cerebral cortex delivery of NMDA in local neurons. Therefore, our findings favored the notion that these neurons may play a vital role in axonal regeneration, synapses, and synaptic plasticity, thus improving the functional recovery of TBI mice.

Acknowledgement

We are grateful to Po Li, Xinyu Zhang, Song Huang, Xiao Han and Likun Yang (Tianjin Medical University, Tianjin, China) for their technical advice.

Funding

This work was supported by the grants from the China Postdoctoral Science Foundation (No. 2019M661042) and the National Natural Science Foundation of China (Nos. 81501071, 31871206 and 31671237).

References

1. Wang G, Zhang YP, Gao Z, Shields LBE, Li F, Chu T, Lv H, *et al*. Pathophysiological and behavioral deficits in developing mice following rotational acceleration-deceleration traumatic brain injury. *Dis Model Mech* 2017, 11: dmm030387
2. Liu SJ, Zou Y, Belegu V, Lv LY, Lin N, Wang TY, McDonald JW, *et al*. Co-grafting of neural stem cells with olfactory ensheathing cells promotes neuronal restoration in traumatic brain injury with an anti-inflammatory mechanism. *J Neuroinflammation* 2014, 11: 66
3. Fu XM, Liu SJ, Dan QQ, Wang YP, Lin N, Lv LY, Zou Y, *et al*. Combined bone mesenchymal stem cell and olfactory ensheathing cell transplantation promotes neural repair associated with CNTF expression in traumatic brain-injured rats. *Cell Transplant* 2015, 24: 1533–1544
4. Robba C, Asgari S, Gupta A, Badenes R, Sekhon M, Bequiri E, Hutchinson PJ, *et al*. Lung injury is a predictor of cerebral hypoxia and mortality in traumatic brain injury. *Front Neurol* 2020, 11: 771
5. Jha RM, Kochanek PM, Simard JM. Pathophysiology and treatment of cerebral edema in traumatic brain injury. *Neuropharmacology* 2019, 145: 230–246
6. Ge L, Zhang C, Xie H, Zhuo Y, Xun C, Chen P, Hu Z, *et al*. A phosphoproteomics study reveals a defined genetic program for neural lineage commitment of neural stem cells induced by olfactory ensheathing cell-conditioned medium. *Pharmacol Res* 2021, 172: 105797
7. Abematsu M, Tsujimura K, Yamano M, Saito M, Kohno K, Kohyama J, Namihira M, *et al*. Neurons derived from transplanted neural stem cells restore disrupted neuronal circuitry in a mouse model of spinal cord injury. *J Clin Invest* 2010, 120: 3255–3266
8. Wang X, Kuang N, Chen Y, Liu G, Wang N, Kong F, Yue S, *et al*.

- Transplantation of olfactory ensheathing cells promotes the therapeutic effect of neural stem cells on spinal cord injury by inhibiting necroptosis. *Aging* 2021, 13: 9056–9070
9. Yokoyama S, Yasui-Furukori N, Nakagami T, Miyazaki K, Ishioka M, Tarakita N, Kubo K, *et al.* Association between the serum carnitine level and ammonia and valproic acid levels in patients with bipolar disorder. *Ther Drug Monit* 2020, 42: 766–770
 10. Xu S, Chen Y, Zhao M, Guo Y, Wang Z, Zhao L. Population pharmacokinetics of valproic acid in epileptic children: effects of clinical and genetic factors. *Eur J Pharmaceutical Sci* 2018, 122: 170–178
 11. Lu J, Xia H, Li W, Shen X, Guo H, Zhang J, Fan X. Genetic polymorphism of GABRG2 rs211037 is associated with drug response and adverse drug reactions to valproic acid in Chinese Southern children with epilepsy. *Pharmacogenomics Pers Med* 2021, 14: 1141–1150
 12. Gu X, Zhu M, Sheng C, Yu S, Peng Q, Ma M, Hu Y, *et al.* Population pharmacokinetics of unbound valproic acid in pediatric epilepsy patients in China: a protein binding model. *Eur J Clin Pharmacol* 2021, 77: 999–1009
 13. Zeng Q, Long Z, Feng M, Zhao Y, Luo S, Wang K, Wang Y, *et al.* Valproic acid stimulates hippocampal neurogenesis via activating the wnt/ β -catenin signaling pathway in the APP/PS1/Nestin-GFP triple transgenic mouse model of Alzheimer's disease. *Front Aging Neurosci* 2019, 11: 62
 14. Kanai H, Sawa A, Chen RW, Leeds P, Chuang DM. Valproic acid inhibits histone deacetylase activity and suppresses excitotoxicity-induced GAPDH nuclear accumulation and apoptotic death in neurons. *Pharmacogenomics J* 2004, 4: 336–344
 15. Sawada K, Kamiya S, Aoki I. The proliferation of dentate gyrus progenitors in the ferret hippocampus by neonatal exposure to valproic acid. *Front Neurosci* 2021, 15: 736313
 16. He H, Li W, Shen B, Zhao H, Liu J, Qin J, Shi J, *et al.* Gene expression changes induced by valproate in the process of rat hippocampal neural stem cells differentiation. *Cell Biol Int* 2020, 44: 536–548
 17. Agrawal SK, Fehlings MG. Role of NMDA and non-NMDA ionotropic glutamate receptors in traumatic spinal cord axonal injury. *J Neurosci* 1997, 17: 1055–1063
 18. Asano D, Morita A, Mori A, Sakamoto K, Ishii K, Nakahara T. Involvement of matrix metalloproteinases in capillary degeneration following NMDA-induced neurotoxicity in the neonatal rat retina. *Exp Eye Res* 2019, 182: 101–108
 19. Rinaldi T, Kulangara K, Antoniello K, Markram H. Elevated NMDA receptor levels and enhanced postsynaptic long-term potentiation induced by prenatal exposure to valproic acid. *Proc Natl Acad Sci USA* 2007, 104: 13501–13506
 20. Long X, Yao X, Jiang Q, Yang Y, He X, Tian W, Zhao K, *et al.* Astrocyte-derived exosomes enriched with miR-873a-5p inhibit neuroinflammation via microglia phenotype modulation after traumatic brain injury. *J Neuroinflammation* 2020, 17: 89
 21. Caudal D, Guinobert I, Lafoux A, Bardot V, Cotte C, Ripoche I, Chalard P, *et al.* Skeletal muscle relaxant effect of a standardized extract of Valeriana officinalis L. after acute administration in mice. *J Traditional Complement Med* 2018, 8: 335–340
 22. Galkov M, Gulyaev M, Kiseleva E, Andreev-Andrievskiy A, Gorbacheva L. Methods for detection of brain injury after photothrombosis-induced ischemia in mice: characteristics and new aspects of their application. *J Neurosci Methods* 2020, 329: 108457
 23. Mohammadian S, Agronskaia AV, Blab GA, van Donselaar EG, de Heus C, Liv N, Klumperman J, *et al.* Integrated super resolution fluorescence microscopy and transmission electron microscopy. *Ultramicroscopy* 2020, 215: 113007
 24. Moon BS, Lu W, Park HJ. Valproic acid promotes the neuronal differentiation of spiral ganglion neural stem cells with robust axonal growth. *Biochem Biophys Res Commun* 2018, 503: 2728–2735
 25. Duan Q, Li S, Wen X, Sunnassee G, Chen J, Tan S, Guo Y. Valproic acid enhances reprogramming efficiency and neuronal differentiation on small molecules staged-induction neural stem cells: suggested role of mTOR signaling. *Front Neurosci* 2019, 13: 867
 26. Codagnone MG, Podestá MF, Uccelli NA, Reinés A. Differential local connectivity and neuroinflammation profiles in the medial prefrontal cortex and hippocampus in the valproic acid rat model of autism. *Dev Neurosci* 2015, 37: 215–231
 27. Samanta D. Epilepsy in Angelman syndrome: a scoping review. *Brain Dev* 2021, 43: 32–44
 28. Wang Y, Liu Y, Lopez D, Lee M, Dayal S, Hurtado A, Bi X, *et al.* Protection against TBI-induced neuronal death with post-treatment with a selective calpain-2 inhibitor in mice. *J Neurotrauma* 2018, 35: 105–117
 29. Choi BY, Lee SH, Choi HC, Lee SK, Yoon HS, Park JB, Chung WS, *et al.* Alcohol dependence treating agent, acamprosate, prevents traumatic brain injury-induced neuron death through vesicular zinc depletion. *Transl Res* 2019, 207: 1–18
 30. Park MK, Choi BY, Kho AR, Lee SH, Hong DK, Jeong JH, Kang DH, *et al.* Effects of transient receptor potential cation 5 (TRPC5) inhibitor, NU6027, on hippocampal neuronal death after traumatic brain injury. *Int J Mol Sci* 2020, 21: 8256
 31. Grovola MR, Paleologos N, Brown DP, Tran N, Wofford KL, Harris JP, Browne KD, *et al.* Diverse changes in microglia morphology and axonal pathology during the course of 1 year after mild traumatic brain injury in pigs. *Brain Pathol* 2021, 31: e12953
 32. Uyeda A, Muramatsu R. Molecular mechanisms of central nervous system axonal regeneration and remyelination: a review. *Int J Mol Sci* 2020, 21: 8116
 33. Qin L, Zou J, Barnett A, Vetreno RP, Crews FT, Coleman Jr. LG. TRAIL mediates neuronal death in AUD: a link between neuroinflammation and neurodegeneration. *Int J Mol Sci* 2021, 22: 2547
 34. Xu C, Wu J, Wu Y, Ren Z, Yao Y, Chen G, Fang EF, *et al.* TNF- α -dependent neuronal necroptosis regulated in Alzheimer's disease by coordination of RIPK1-p62 complex with autophagic UVRAG. *Theranostics* 2021, 11: 9452–9469
 35. Oraee-Yazdani S, Akhlaghasand M, Golmohammadi M, Hafizi M, Zomorrod MS, Kabir NM, Oraee-Yazdani M, *et al.* Combining cell therapy with human autologous Schwann cell and bone marrow-derived mesenchymal stem cell in patients with subacute complete spinal cord injury: safety considerations and possible outcomes. *Stem Cell Res Ther* 2021, 12: 445
 36. Wu J, Zhu ZY, Fan ZW, Chen Y, Yang RY, Li Y. Downregulation of EphB2 by RNA interference attenuates glial/fibrotic scar formation and promotes axon growth. *Neural Regen Res* 2022, 17: 362–369
 37. Zou HJ, Guo SW, Zhu L, Xu X, Liu JB. Methylprednisolone induces neuroprotective effects via the inhibition of a1 astrocyte activation in traumatic spinal cord injury mouse models. *Front Neurosci* 2021, 15: 628917
 38. Yang Y, Gao L, Niu Y, Li X, Liu W, Jiang X, Liu Y, *et al.* Kukoamine a protects against NMDA-induced neurotoxicity accompanied with down-regulation of GluN2B-containing NMDA receptors and phosphorylation of PI3K/Akt/GSK-3 β signaling pathway in cultured primary cortical neurons. *Neurochem Res* 2020, 45: 2703–2711
 39. Yang X, Zhang H, Wu J, Yin L, Yan LJ, Zhang C. Humanin attenuates NMDA-induced excitotoxicity by inhibiting ROS-dependent JNK/p38 MAPK pathway. *Int J Mol Sci* 2018, 19: 2982
 40. Sone K, Mori A, Sakamoto K, Nakahara T. GYY4137, an extended-release

- hydrogen sulfide donor, reduces NMDA-induced neuronal injury in the murine retina. *Biol Pharmaceutical Bull* 2018, 41: 657–660
41. Watanabe K, Asano D, Ushikubo H, Morita A, Mori A, Sakamoto K, Ishii K, *et al.* Metformin protects against NMDA-induced retinal injury through the MEK/ERK signaling pathway in rats. *Int J Mol Sci* 2021, 22: 4439
 42. Ziemens D, Oschmann F, Gerkau NJ, Rose CR. Heterogeneity of activity-induced sodium transients between astrocytes of the mouse hippocampus and neocortex: mechanisms and consequences. *J Neurosci* 2019, 39: 2620–2634
 43. Postnikova TY, Trofimova AM, Ergina JL, Zubareva OE, Kalemenev SV, Zaitsev AV. Transient switching of NMDA-dependent long-term synaptic potentiation in CA3-CA1 hippocampal synapses to mGluR1-dependent potentiation after pentylenetetrazole-induced acute seizures in young rats. *Cell Mol Neurobiol* 2019, 39: 287–300
 44. Laliberte AM, Goltash S, Lalonde NR, Bui TV. Proprio-spinal neurons: essential elements of locomotor control in the intact and possibly the injured spinal cord. *Front Cell Neurosci* 2019, 13: 512
 45. Brommer B, He M, Zhang Z, Yang Z, Page JC, Su J, Zhang Y, *et al.* Improving hindlimb locomotor function by Non-invasive AAV-mediated manipulations of proprio-spinal neurons in mice with complete spinal cord injury. *Nat Commun* 2021, 12: 781
 46. Ramadan E, Basselin M, Rao JS, Chang L, Chen M, Ma K, Rapoport SI. Lamotrigine blocks NMDA receptor-initiated arachidonic acid signalling in rat brain: implications for its efficacy in bipolar disorder. *Int J Neuropsychopharm* 2012, 15: 931–943
 47. Kimura A, Namekata K, Guo X, Noro T, Harada C, Harada T. Valproic acid prevents NMDA-induced retinal ganglion cell death via stimulation of neuronal TrkB receptor signaling. *Am J Pathol* 2015, 185: 756–764
 48. Park HJ, Kang WS, Paik JW, Kim JW. Effect of valproic acid through regulation of NMDA receptor–ERK signaling in sleep deprivation rats. *J Mol Neurosci* 2012, 47: 554–558
 49. Hsu SW, Hsu PC, Chang WS, Yu CC, Wang YC, Yang JS, Tsai FJ, *et al.* Protective effects of valproic acid on 6-hydroxydopamine-induced neuroinjury. *Environ Toxicol* 2020, 35: 840–848